

# The wetting behavior of NiAl and NiPtAl on polycrystalline alumina

A. Gauffier<sup>+</sup>, E. Saiz, A. P. Tomsia and P. Y. Hou

Materials Sciences Division  
Lawrence Berkeley National Laboratory  
Berkeley, CA 94720, USA

<sup>+</sup>Ecole de Mines d'Albi-Carmaux  
Campus Jarlard- route de Teillet  
Albi, CT Cedex 09, France

## ABSTRACT

In order to understand the beneficial effect of Pt on the adherence of thermally grown alumina scales, sessile drop experiments were performed to study the wetting of poly-crystalline alumina by nickel-aluminum alloys with or without platinum addition where the amount of Pt ranged from 2.4 to 10 at.%. Subsequent interfacial structure was evaluated using atomic force microscopy. Platinum addition enhances the wettability of NiAl alloys on alumina, reduces the oxide/alloy interface energy and increases the interfacial mass transport rates.

## INTRODUCTION

Metal/oxide interfaces are involved in many technologically relevant systems [1, 2]. One example that is of particular interest to this work is the critical interface that forms between  $\text{Al}_2\text{O}_3$  and its underlying alloy or coating when the metal is exposed at elevated temperatures. The reason this interface is *critical* is because failure often occurs there due to poor oxide-metal adhesion. Such failure can affect the metal component that the  $\text{Al}_2\text{O}_3$  scale is supposed to protect from continued oxidation attack. Even worse, it can cause thermal barrier coatings (TBC's), which are deposited on top  $\text{Al}_2\text{O}_3$ -forming alloys or coatings, to spall with it.

There are three well known methods for improving the alumina layer adherence: addition of a reactive element, such as Y, Hf or Zr [3], reduction of sulphur impurity in the alloy, and alloying with precious metals, in particular Pt [4-6]. In fact, the oxidation performance of commercial aluminide coatings has been enhanced by platinum additions during the last 30 years [7], but the mechanism of the Pt effect are still unknown. While the high sulphur affinity of a reactive element may prevent sulphur segregation to the oxide/metal interface and the associated decrease of strength [8], the same is not expected for Pt, because the heat of formation for a reactive element sulfide is 3-5 times greater than that of Pt sulfide, and Pt sulfide is even less stable than Al sulfide [9, 10].

The goal of this study is to understand the beneficial effect of Pt on Al<sub>2</sub>O<sub>3</sub> scale adhesion by evaluating how Pt affects the Al<sub>2</sub>O<sub>3</sub>/NiAl interface. Wetting experiments of alumina by nickel-aluminium alloys and nickel-aluminium-platinum alloys with the sessile drop method [11] are used. Although usual oxidation temperatures (1100-1200°C) are much lower than those at which the experiments are conducted (1650°C), this method was chosen because liquid wetting experiments are the only probe we have to experimentally measure basic interfacial thermodynamic quantities such as the work of adhesion [12]. Furthermore, characterization of the interface structure, i.e., grain boundary grooves, after the wetting experiments offers insights into the interface energies and its mass transport properties [13-20].

## EXPERIMENTAL METHODS

The alloys used in this study were (in at.%): Ni-25Al, Ni-37Al, Ni-37Al-5Pt, Ni-37Al-10Pt, Ni-40Al, Ni-50Al, Ni-50Al-2.4Pt and Ni-50Al-10Pt. All alloys were made with high-purity constituent metals into 7×1.3 mm bars. Most of them, except for the Ni-40Al and the Ni-50Al-2.4Pt, were fabricated at Ames National Laboratory into drop-cast bars by argon-arc melting; the as-cast bars were heat treated in argon for 6h at 1200°C, then 48h at 1150°C. The Ni-50Al-2.4Pt was made at Oak Ridge National Lab by induction melting, followed by annealing at 1300°C for 4h. The Ni-40Al was made at Lawrence Berkeley National Lab by arc-melting, followed by heat treatment at 1150°C for 15h. Test coupons approximately 1 mm in diameter were cut from the bars, and then further cut into 2 mm<sup>3</sup> pieces for wetting studies. Polycrystalline alumina (99.999 %, Showa-Denko, Japan) substrates with average grain size of approximately 20 μm were prepared following a procedure described in detail elsewhere [13]. The alloy pieces, before the wetting experiments, were roughly grounded on 240 grit SiC to remove surface oxides. The alloy and alumina substrates were then cleaned ultrasonically in acetone, followed by ethanol and then distilled water.

Wetting experiments were performed by melting the pieces of Ni-Al or Ni-Al-Pt alloy on polycrystalline alumina substrates in a small closed alumina crucible. Under this condition, the equilibrium oxygen partial pressure,  $p(\text{O}_2)^{\text{eq}}$ , inside the crucible is close to the phase boundary value at which Al and Al<sub>2</sub>O<sub>3</sub> coexist in equilibrium [14-16]. Tests were conducted in a vacuum furnace under  $5 \times 10^{-6}$  Torr. The heating rate was 25°C/min up to 1650°C, and then the temperature was maintained for 1h at 1650°C, which is above the highest melting point of the alloy studied, (1638°C for Ni-50Al). After 1h, the furnace power was turned off. Contact angles between each alloy and the alumina were measured after cool down using a goniometer. A few test samples, after mechanically or chemically removing the alloy droplet, were studied using Atomic Force Microscopy (AFM) to examine the alumina grain boundary grooves beneath the droplet.

## RESULTS AND DISCUSSION

Platinum additions to the β-NiAl alloys were found to decrease the contact angle for a given Al content by about 6% and the reduction is independent of the amount of Pt added, from 2.4 to 10 at% (Fig. 1, where data from refs [13, 17, 18] are also included for

comparison). This result suggests that platinum additions improve the wettability between the alloys and alumina, and this should improve interfacial bonding.

Metal/oxide interfaces such as Ni/Al<sub>2</sub>O<sub>3</sub> are in fact ternary systems for which the oxygen activity is a fundamental variable. The Ni/Al<sub>2</sub>O<sub>3</sub> couple can coexist in equilibrium over a range of  $p(\text{O}_2)$ . In this compatibility range, the composition of the bulk phases can change and, due to adsorption, the surface and interfacial energies and the contact angle can vary with oxygen activity [19, 20]. When the oxygen activity in the system is decreased (or the Al activity increased), the content of Al in the liquid in equilibrium with Al<sub>2</sub>O<sub>3</sub> increases, since in the presence of alumina  $a_{\text{Al}}^2 a_{\text{O}}^3 = K(T)$  ( $a_{\text{Al}}$  and  $a_{\text{O}}$  being the Al and oxygen activities, respectively). As a consequence, at temperatures high enough for all compositions in the binary system Ni-Al to be molten, the composition of the liquid in equilibrium with alumina is nearly pure Al at the low  $p(\text{O}_2)$  phase boundary and increases rapidly in its Ni content with rising oxygen activity, resulting in an increase in the contact angle and the surface and interface energies [13, 19, 21].

In the inside of our small closed crucible, the oxygen activity is expected to be fixed by the solid/liquid interactions to that of the equilibrium value between the corresponding Ni/Al or Ni/Al/Pt liquid and the alumina. Since Pt addition has been shown to decrease Al activity [22], thus increasing the  $p(\text{O}_2)$ , higher contact angles for the Ni-Pt-Al system should be expected. However, our results show a decreased contact angle, indicating that the effect of Pt on wetting is beyond that of affecting the Al activity.

According to the Young's equation  $\gamma_{\text{iF}} = \gamma_{\text{ox}} - \gamma_{\text{m}} \cos \theta$  where  $\gamma_{\text{ox}}$ ,  $\gamma_{\text{iF}}$  and  $\gamma_{\text{m}}$  are, respectively, the oxide surface, the metal/oxide interface and the metal surface energies. While it has been observed that at high temperature the formation of ridges could preclude this interpretation of the contact angle [23, 24], this complication should not apply here, because when the ridge is small compared with the radius of the drop, the contact angle still tends towards a value close to that given by the Young's equation. The surface energies of the alloys,  $\gamma_{\text{m}}$ 's, were not determined in this study, because  $\gamma_{\text{m}}$  can only be accurately evaluated using the sessile drop method when the liquid does not wet the solid, i.e.,  $\theta$  being greater than 90°. However, a recent study by first principles calculation [25] showed that Pt addition in  $\beta$ -NiAl noticeably increases the alloy surface energy. Therefore, since Pt reduces  $\theta$ , and increases  $\gamma_{\text{m}}$ , Pt should decrease the metal/oxide interface energy. In terms of interface strength, the lower  $\gamma_{\text{iF}}$  and the increase in  $\gamma_{\text{m}}$  caused by Pt addition should increase the work of adhesion,  $W_{\text{ad}} = \gamma_{\text{ox}} + \gamma_{\text{m}} - \gamma_{\text{iF}}$ . [25].

From Fig. 2, the alumina outside the alloy's drop is seen to be strongly faceted whereas the area inside the drop is not, suggesting that the solid/liquid interface is more isotropic than the solid/gas interface. The measured  $\Phi$  for alumina outside the drop is  $\sim 148^\circ$  independently of the liquid composition (Table 1), and the width ranges between 1.8-2.0  $\mu\text{m}$ . Grain boundary grooves at the solid/liquid (inside the drop) interfaces are noticeably wider and deeper than those at the solid/vapour (outside the drop) interfaces. The addition of Pt decreases the measured dihedral angle and increases the depth and width of the grain boundary grooves at the solid/liquid interface (Table 1); the decrease of

dihedral angle may be greater with higher concentrations of Pt in the alloy. The grain boundary grooves under the Pt-containing alloys were always more symmetrically shaped than those under the alloy without platinum, in that the humps on either side of the groove were more even. This could mean that the  $\text{Al}_2\text{O}_3/\text{Ni-Al-Pt}$  interfaces are more isotropic than the  $\text{Al}_2\text{O}_3/\text{Ni-Al}$  interfaces.

A decrease in dihedral angle could be the consequence of a reduced interfacial energy. By definition, the dihedral angle,  $\Phi$ , is the equilibrium angle that forms when a boundary intersects an interface where  $\gamma_{gb} = 2\gamma_{iF} \cos(\Phi/2)$ ;  $\gamma_{gb}$  in our case is the grain boundary energy of the alumina. It has been shown for metal/alumina systems that dihedral angles for grooves narrower than  $5 \mu\text{m}$  can be overestimated from AFM measurements, because the tip can not always penetrate close enough to the root of the groove [13]. Therefore, the true dihedral angles should be larger than those values reported in Table 1. Nevertheless, since the grain boundary widths did not vary much between the alloys, the data can be trusted in comparison, whereby the effect of Pt is consistently shown to lower the dihedral angle.

The decrease by Pt of the interfacial energy  $\gamma_{iF}$  may explain why sulphur impurity does not segregate to the interfaces between thermally grown  $\text{Al}_2\text{O}_3$  and Pt-containing Ni-Al alloys [26]. Since the driving force for segregation is directly related to the interface or surface energy [27], a lower energy would result in less segregation. Although this is a reasonable explanation, it should be noted that Pt also reduced sulphur segregation to alloy surfaces [26, 28], while by first principles calculation [25], Pt increases the alloy's surface energy. Therefore, the reason why Pt reduces S segregation to NiPtAl surfaces and prevents segregation at  $\text{Al}_2\text{O}_3/\text{NiPtAl}$  interfaces [26] is still not resolved. It is possible that Pt reduces the S activity in the alloy, not by forming a sulphide like the reactive elements, but perhaps by increasing the S solubility.

The grain boundary groove profiles at the solid-liquid and solid-vapor interfaces (Fig. 3), show humps on either side of the roots which indicate that the kinetics are limited by diffusion, rather than the dissolution/precipitation rates. Diffusion occurs through two paths: the volume of the liquid or solid phase and through the surface. Transport of the  $\text{Al}_2\text{O}_3$  involves diffusion of both Al and O ions or atoms. Although each specie could move independently along either path, the dissolution and deposition must involve stoichiometric  $\text{Al}_2\text{O}_3$  and the movement of the slowest specie through the fastest path will control the kinetics of groove evolution. Grooving is much faster under the drop, where the fastest path is metal volume diffusion through the liquid [13, 29]. The measured groove widths can be used to estimate the volume diffusivity ( $xD_v$ , where  $x$  is the molar solubility and  $D_v$  is the volume diffusion coefficient) of the controlling species [13, 30-32]. The corresponding volume diffusivities are of the order of  $10^{-13} \text{ m}^2 \cdot \text{s}$ , close to what has been observed in similar systems [13]. If the diffusion coefficient in the liquid is  $D_v \approx 10^{-9} \text{ m}^2 \cdot \text{s}^{-1}$  (a typical value for liquid metals) [33], the estimated solubility of the slow species (Al or O-rich species) in the liquid droplet is  $\sim 10^{-4}$ . This is of the order of those measured for Ni/ $\text{Al}_2\text{O}_3$  interfaces [13].

The presence of Pt in Ni-Al liquid is also found to increase slightly the width and depth of the grain boundary grooves, suggesting an enhanced mass transport rate with the presence of Pt. Because the liquids have very large quantities of Al (from the dissolved Ni-Al alloys) compared to O, oxygen rich species should control the kinetics of grain boundary grooving in these systems. Pt is known to reduce Al activity [22] and consequently increase oxygen activity; in this way it will increase the controlling diffusivity resulting in faster grooving.

In the surface of alumina outside the drop the grooving kinetics will be controlled by surface diffusion. The calculated surface diffusivity for the slowest species are of the order or  $10^{-20} \text{ m}^3\cdot\text{s}$ , which is slightly larger than rates typically reported for alumina at these temperatures [13, 30, 31, 32, 34]. However, the diffusivities measured in this work correspond to Al rich surfaces while most of the published data has been measured for much larger oxygen activities.

## CONCLUSIONS

Wetting experiments using the sessile drop method were performed for different compositions of nickel-aluminum alloys (with or without platinum additions) on polycrystalline alumina substrates. Platinum was found to improve the wettability, reduce the metal/ceramic interfacial energy and increase the work of adhesion between  $\text{Al}_2\text{O}_3$  and Ni-Al alloys. Platinum additions also increased the mass transport rates at the interface between the liquid Ni-Al alloys and alumina, and resulted in more isotropic interfaces.

## ACKNOWLEDGMENT

The authors thank Ms. Kunie Priimak for assistance with some of the experimental work, and Prof. Brian Gleeson of Iowa State University and Dr. Bruce Pint of Oak Ridge National Lab for supplying alloys. This work was supported by the Director, Office of Science, Office of Basic Energy Sciences, Materials Sciences and Engineering Division, of the U.S. Department of Energy under Contract No. DE-AC02-05CH11231.

## REFERENCES

- [1] M. Rühle, Metal-ceramic interfaces: proceedings of an international workshop, Santa Barbara, California, USA, 16-18 January 1989, Pergamon, Oxford; New York, 1990.
- [2] J. S. Moya, S. Lopez-Esteban and C. Pecharromás, *Progress in Materials Science*, available on line [doi:10.1016/j.pmatsci.2006.09.003](https://doi.org/10.1016/j.pmatsci.2006.09.003) (2007).
- [3] D. P. Whittle and J. Stringer, *Philosophical Transactions of the Royal Society of London Series a-Mathematical Physical and Engineering Sciences*, 295 (1980), p. 309.
- [4] E. J. Felten, *Oxidation of Metals*, 10 (1976), p. 23.

- [5] J. A. Haynes, K. L. More, B. A. Pint, I. G. Wright, K. Cooley and Y. Zhang, *High Temperature Corrosion and Protection of Materials 5, Pts 1 and 2*, 369-3 (2001), p. 679.
- [6] Y. Zhang, J. A. Haynes, W. Y. Lee, I. G. Wright, B. A. Pint, K. M. Cooley and P. K. Liaw, *Metall Mater Trans A*, 32 (2001), p. 1727.
- [7] R. Lowrie and D. H. Boone, *Thin Solid Films*, 45 (1977), p. 491.
- [8] A. W. Funkenbusch, J. G. Smeggil and N. S. Bornstein, *Metallurgical Transactions a-Physical Metallurgy and Materials Science*, 16 (1985), p. 1164
- [9] D. R. Sigler, *Oxidation of Metals*, 32 (1989), p. 337.
- [10] CRC handbook of chemistry and physics, CRC Press, Boca Raton, Fla., 1990.
- [11] N. Sobczak, M. Singh and R. Asthana, *Current Opinion in Solid State & Materials Science*, 9 (2005), p. 241-253.
- [12] N. Eustathopoulos, N. Sobczak, A. Passerone and K. Nogi, *Journal of Materials Science*, 40 (2005), p. 2271.
- [13] E. Saiz, R. M. Cannon and A. P. Tomsia, *Acta Materialia*, 47 (1999), p. 4209.
- [14] E. Ricci and A. Passerone, *Materials Science and Engineering A-Structural Materials Properties Microstructure and Processing*, 161 (1993), p. 31.
- [15] E. Ricci, E. Arato, A. Passerone and P. Costa, *Advances in Colloid and Interface Science*, 117 (2005), p. 15.
- [16] E. Saiz, A. P. Tomsia and K. Suganuma, *Journal of the European Ceramic Society*, 23 (2003), p. 2787.
- [17] V. Merlin and N. Eustathopoulos, *Journal of Materials Science*, 30 (1995), p. 3619.
- [18] E. Saiz, R. M. Cannon and A. P. Tomsia, unpublished work.
- [19] E. Saiz, A. P. Tomsia and R. M. Cannon, in: A. P. Tomsia and A. M. Glaeser (Eds.), Plenum Press, New York, 1998, pp. 65-82.
- [20] D. Chatain, F. Chabert, V. Ghetta and J. Fouletier, *Journal of the American Ceramic Society*, 77 (1994), p. 197.
- [21] G. Levi, D. R. Clarke and W. D. Kaplan, *Interface Science*, 12 (2004), p. 73.
- [22] S. Hayashi, W. Wang, D. J. Sordelet and B. Gleeson, *Metall Mater Trans A*, 36A (2005), p. 1769.
- [23] E. Saiz, A. P. Tomsia and R. M. Cannon, *Acta Materialia* (1998), p. 2349.
- [24] E. Saiz, A. P. Tomsia and R. M. Cannon, *Scripta Materialia*, 44 (2001), p. 159.
- [25] R. Yu and P. Y. Hou, paper submitted to *Appl. Phys. Lett.*
- [26] P. Y. Hou and K. F. McCarty, *Scripta Materialia*, 54 (2006), p. 937-941.
- [27] J. de Plessis, *Diffusion and Deflect Data-Solid State Phenomena*, Sci-Tech Publish, Liechtenstein, 1990.

- [28] Y. Cadoret, M. P. Bacos, P. Josso, V. Maurice, P. Marcus and S. Zanna, *High Temperature Corrosion and Protection of Materials 6, Prt 1 and 2, Proceedings*, 461-464 (2004), p. 247-254.
- [29] A. H. Feingold and C. Y. Li, *Acta Metallurgica*, 16 (1968), p. 1101.
- [30] W. W. Mullins, *Journal of Applied Physics*, 28 (1957), p. 333.
- [31] W. W. Mullins, *Transactions of the American Institute of Mining and Metallurgical Engineers*, 218 (1960), p. 354.
- [32] W. W. Mullins and P. G. Shewmon, *Acta Metallurgica*, 7 (1959), p. 163.
- [33] C. J. Smithells and E. A. Brandes, *Metals reference book*, Butterworths, London; Boston, 1976.
- [34] J. M. Dynys, R. L. Coble, W. S. Coblenz and C. R. M., in: G. C. Kuczynski (Eds.), *Plenum Press*, New York, 1980, pp. 391.

Table 1: Average dihedral angle measured by AFM traces from grain boundaries of  $\text{Al}_2\text{O}_3$  after wetting experiments.

Alloy	Inside the drop			Outside the drop		
	Dihedral Angle ( $^\circ$ )	Width ( $\mu\text{m}$ )	Depth (nm)	Dihedral Angle, $\Phi$	Width ( $\mu\text{m}$ )	Depth (nm)
Ni-37Al	$147.2 \pm 4.1$	$3.2 \pm 0.5$	$261 \pm 47$	$150.6 \pm 5.8$	$2.0 \pm 0.4$	$146 \pm 51$
Ni-37Al-5Pt	$140.2 \pm 6.2$	$3.4 \pm 0.4$	$286 \pm 38$	$146.4 \pm 4.0$	$1.8 \pm 0.4$	$146 \pm 28$
Ni-37Al-10Pt	$136.9 \pm 5.7$	$3.5 \pm 0.3$	$337 \pm 46$	$147.2 \pm 7.5$	$1.9 \pm 0.3$	$159 \pm 52$



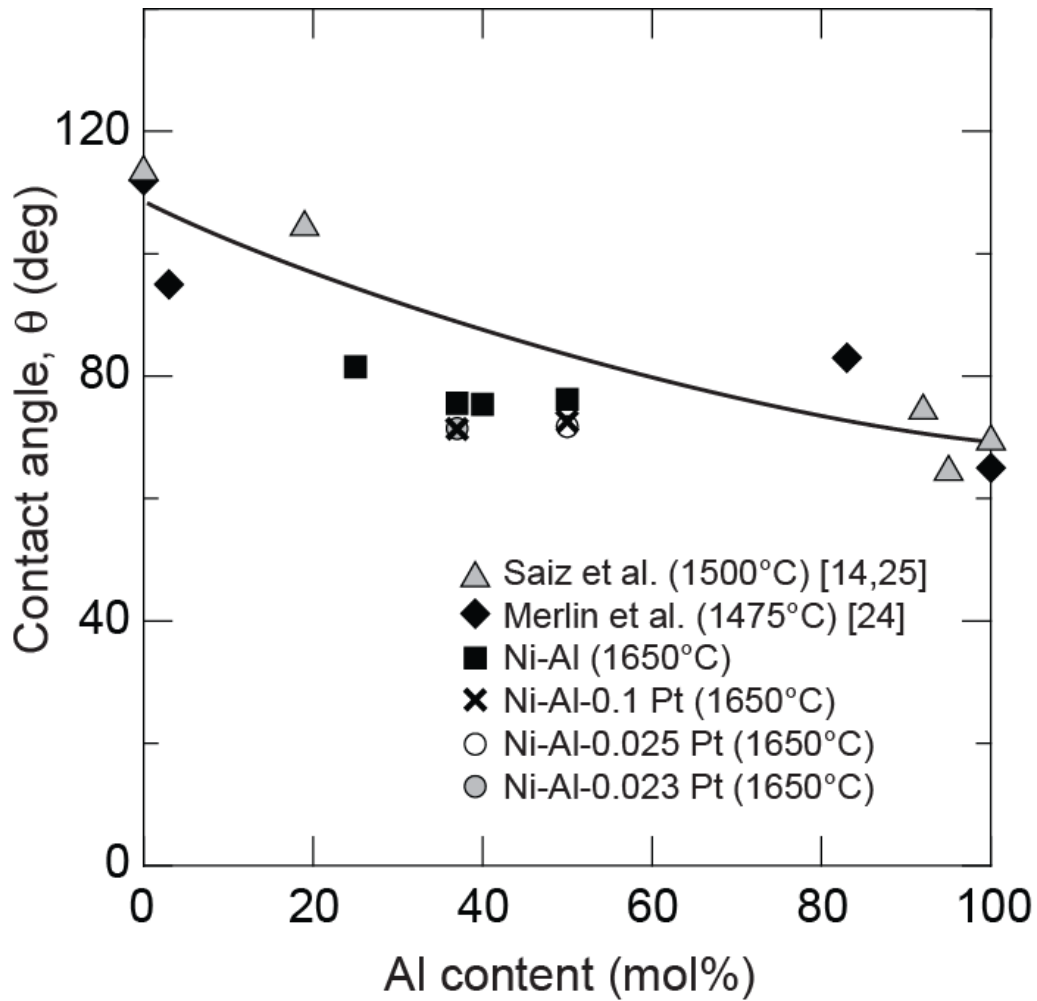


Figure 1: Relationship between contact angle and the aluminum concentration. The data for pure Ni is taken under conditions in which no oxygen adsorption is expected on the metal surface (either high vacuum or purified He). Since the three sets of data for Ni-xAl were performed at different temperatures, there is some degree of scattering. Nevertheless all data follows a similar trend and it appears that increasing the aluminium concentration leads to a decrease of the contact angle.

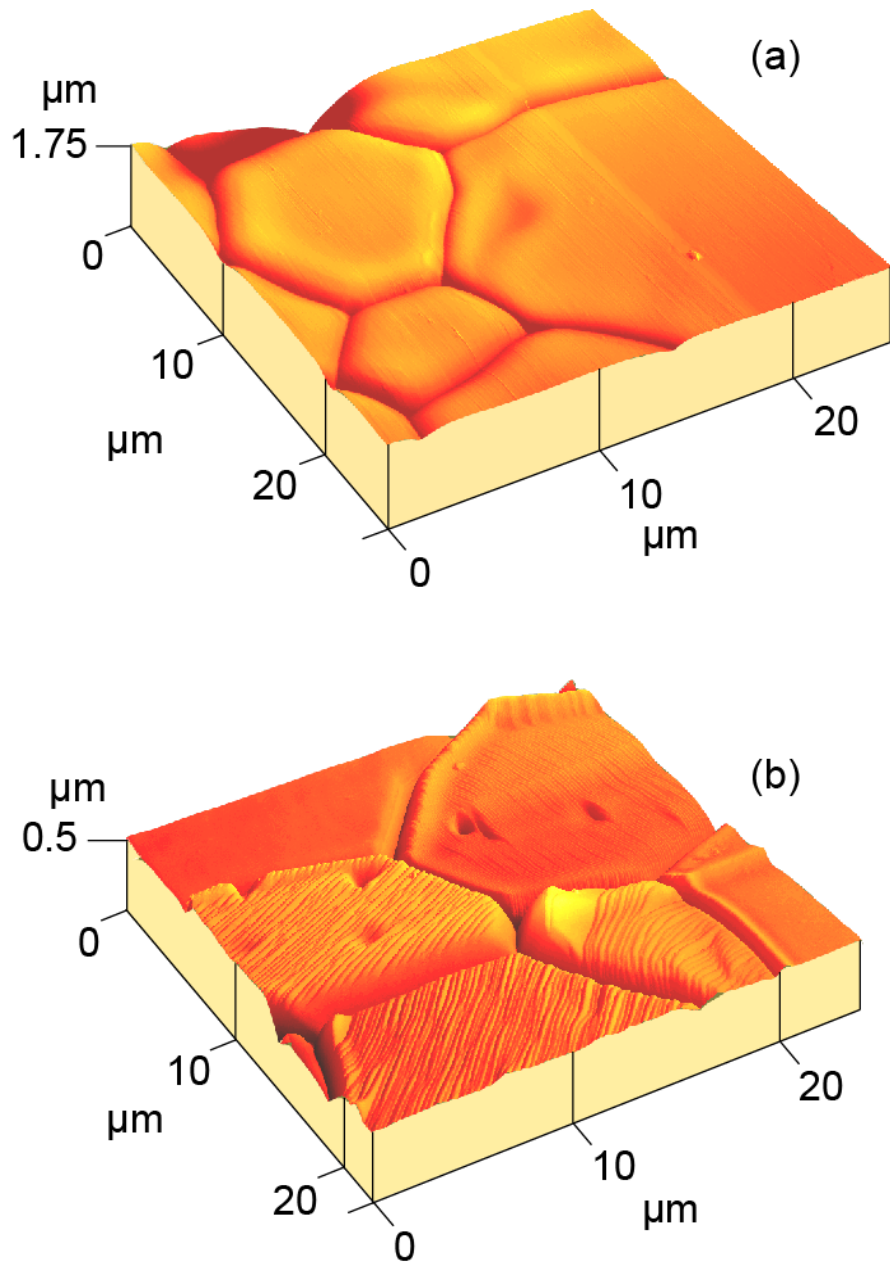


Figure 2: Three dimensional AFM scans (constant force mode) of an  $\text{Al}_2\text{O}_3$  area (a) under and (b) outside the Ni-37Al-5Pt droplet.

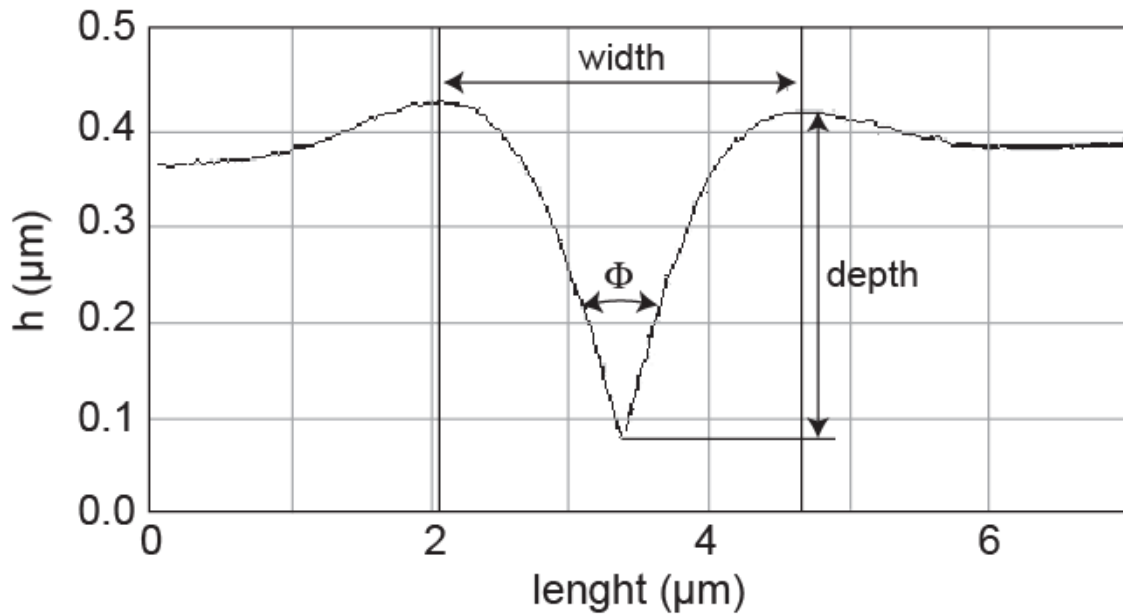


Figure 3: AFM line trace across an alumina grain boundary inside the wetting droplet showing measurements of boundary dihedral angle, width and depth. The dihedral angle is the angle between two tangents drawn on the grain boundary groove; the width is defined as the distance between the two highest points on each side of the boundary, and the depth is the distance from these highest points to the lowest point of the groove.